Growth of SiC polytypes by the physical vapour transport technique

2004 J. Phys.: Condens. Matter 16 S1597

(http://iopscience.iop.org/0953-8984/16/17/010)

INSTITUTE OF PHYSICS PUBLISHING JOURNAL OF PHYSICS: CONDENSED MATTER

J. Phys.: Condens. Matter **16** (2004) S1597–S1610 PII: S0953-8984(04)65142-3

Growth of SiC polytypes by the physical vapour transport technique

K Semmelroth, N Schulze[1] and G Pensl

Institute of Applied Physics, University of Erlangen-Nürnberg, Staudtstrasse 7, DE-91058 Erlangen, Germany

E-mail: gerhard.pensl@physik.uni-erlangen.de

Received 24 June 2003
Published 16 April 2004
Online at stacks.iop.org/JPhysCM/16/S1597
DOI: 10.1088/0953-8984/16/17/010

Abstract

A brief survey of the development of the sublimation growth of SiC is given. The growth equipment and especially the hot zone of the furnace for the physical vapour transport (PVT) technique are described in detail. In order to grow micropipe-free SiC crystals, near-thermal-equilibrium growth is developed and the individual processing steps are revealed. The essential parameters for the growth of 4H-, 6H-, 15R- and 3C-SiC single crystals are discussed and a survey of the incorporation of donors (N, P) and acceptors (Al, B) during the PVT growth is presented.

1. Introduction: a brief survey of the growth of SiC bulk crystals from the vapour phase

The technical importance of SiC as a grinding and cutting material was realized during the last decades of the 19th century [1, 2]. For this application, SiC material has been and is still fabricated by the Acheson process [3], which is based on a reduction of silica (SiO_2) by carbon (C) at temperatures above 2000 °C. This SiC material is highly contaminated and, therefore, not suitable for the fabrication of electronic devices.

A major step in the growth of pure SiC crystals was taken by Lely [4] at Philips in Eindhoven, who made use of the property of SiC that it does not melt but sublimes at elevated temperatures and normal pressure. Assuming that in a closed vessel the partial pressure of the most volatile components (e.g. Si, SiC_2, Si_2C) of the dissociating SiC is equal to the corresponding equilibrium pressure at a certain temperature, a mass transport of these components can be achieved from a hotter to a colder part in the vessel resulting in the growth of SiC crystals in the colder part. The shape of such platelets corresponds to flat pyramids with a hexagonal basal plane. These crystals are a few millimetres in height and about 1 cm in diameter (see figure 1). The Lely platelets are known for their high crystalline quality, that means low density of extended crystal defects and high polytype purity.

[1] Present address: Infineon Technologies Dresden, Königsbrücker Straße 180, DE-01099 Dresden, Germany.

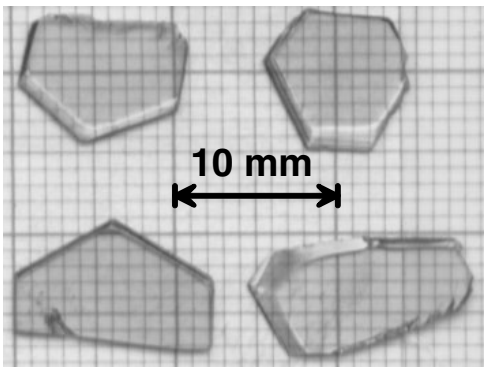

Figure 1. Lely platelets sliced from crystals, which are grown by the original Lely method.

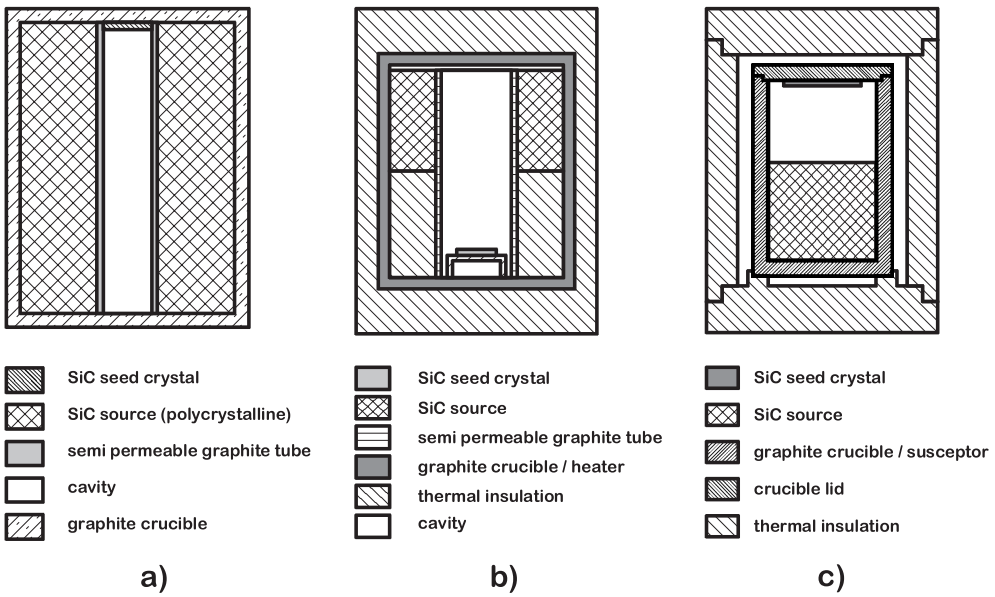

Figure 2. 'Modified Lely method' according to (a) Tairov and Tsvetkov [6] with the seed mounted at the lid of the crucible and the source material separated from the inner growth chamber by a semi-permeable graphite membrane, (b) Ziegler *et al* [7] with the seed mounted at the bottom and the source material located in the upper half of the crucible and (c) Augustine *et al* [8] with the seed mounted at the lid of the crucible and the source material located directly at the bottom of the growth chamber.

First attempts to improve the sublimation growth by using a seed crystal were made by Hergenrother *et al* [5] at the beginning of the 1960s. However, it took almost another two decades until a successful 'seeded' Lely growth was reported in the literature [6]; this technique is called the 'modified Lely method' or 'physical vapour transport (PVT)' technique. Regarding the position of the SiC source material and SiC seed in the growth furnace, several arrangements were developed; they are schematically shown in figure 2. Tairov and Tsvetkov [6] mounted the seed crystal at the lid of the graphite crucible; the polycrystalline SiC source material was separated from the inner growth chamber by a semi-permeable graphite tube (see figure 2(a)). The temperature of the source material was varied between 1800 and 2600 °C

and the temperature gradient to the seed was $dT/dx \approx -30$ K cm^{-1}. Most of the grown crystals were of the 6H-polytype (a few also from the 4H- or 15R-polytype). Ziegler *et al* [7] with Siemens Research Laboratories fixed the seed crystal at the bottom of the inner cylinder (see figure 2(b)) and the source material was stored in the upper half of the crucible. These authors maintained a pressure of 2 mbar argon in the inner growth chamber and used a source temperature of 2200 °C and a temperature gradient of $dT/dx = -20$ K cm^{-1}. A typical result of such a growth run was a 6H-SiC single crystal of 85% polytype purity and 14–20 mm in diameter. A certain disadvantage of this arrangement is the position of the seed crystal, which is fixed at the bottom. Graphite particles can easily be deposited at the growth front, which may develop to nucleation seeds for extended defects. At Westinghouse D L Barrett and colleagues [8], therefore, modified the PVT technique; they fixed the seed at the lid of the crucible and filled the SiC source material directly into the lower part of the inner cylinder (see figure 2(c)). This arrangement was extremely successful in extending the diameter of the grown SiC crystals (≈50 mm) and in reducing extended crystal defects like so-called micropipes (see section 3) or inclusions. Nowadays this growth set-up is used worldwide.

Alternatively, Vodakov *et al* [9] used a sublimation sandwich system to grow thick SiC layers on SiC seed crystals. In this system, the inner container consists of tantalum (Ta); its surface is transformed into TaC, which is chemically stable up to 3000 °C. The seed is placed close to the source material and a temperature gradient of −(1–5) K cm^{-1} between source and seed is maintained. With this growth technique, SiC crystals of 20 mm in height are grown with low micropipe density.

In the following sections, we report experimental details of the PVT growth, specify conditions for the growth of a particular polytype and describe the possibility of doping SiC crystals during growth with donors or acceptors.

2. Physical vapour transport technique

2.1. Principle of sublimation growth

The mechanism of growth by sublimation can be subdivided into three successively proceeding steps:

- sublimation of the SiC powder source forming a gaseous phase [10, 11],
- transport of the gaseous species from the source to the growth front, which is governed by diffusion and advection (Stefan flow) [12–14] and
- incorporation of the gaseous species into the surface layer of the growing crystal [15].

The step with the largest time constant determines the growth rate of the crystal. Tairov and Tsvetkov [16] report that the growth rate is predominantly governed by the mass transport in the gas phase.

2.2. Sublimation growth furnace

The growth system [17] employed at our institute corresponds to the system developed at Westinghouse (see figure 3). The growth furnace is located in a double-walled quartz glass tube, which is cooled with water. The susceptor is heated by an induction coil, which is powered by an HF generator (power $\leqslant$ 50 kW, frequency $\leqslant$ 250 kHz). The temperature of the graphite crucible is determined at the top and at the bottom by two differential pyrometers. The crucible can be evacuated to a pressure of 10^{-8} mbar and a gas supply through a needle valve provides the possibility to fill the crucible with an inert and/or dopant gas at low pressure.

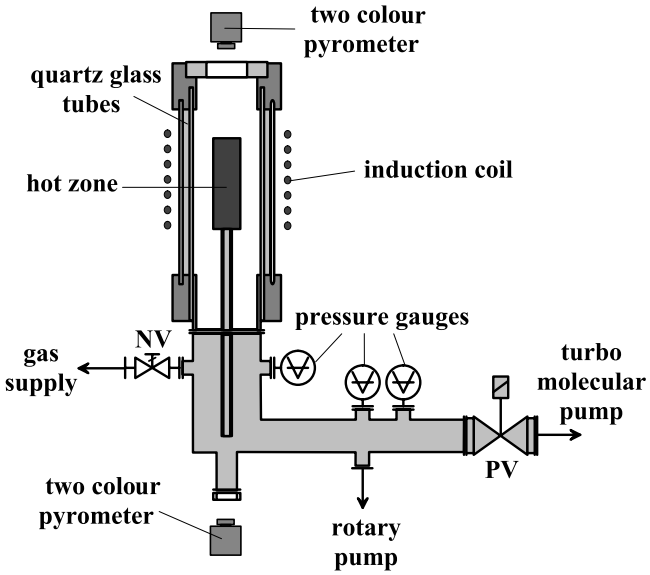

Figure 3. Schematic overview of the sublimation furnace for the growth of SiC single crystals by the PVT method (after [17]).

The system can be operated under gas flow or static conditions; the growth runs discussed in this paper are conducted under static conditions.

The inner part of the Lely furnace is shown in figure 4 (see [18]). All parts are made of solid graphite, except the thermal insulation cylinder, which is made of graphite foam. The susceptor absorbs the electrical HF field and heats the crucible by radiation. The discs and the position of the coil adjust the temperature gradient. The distance between source and seed is about 30 mm and the inner diameter of the crucible is 25 mm in our furnace. For special doping experiments (aluminium (Al) or phosphorus (P)), a solid dopant source has been used. Because of the high vapour pressure of all the suitable Al and P compounds, the dopant source has to be placed at lower temperature. The evaporating dopant gas is connected to the growth front by tubes drilled through the graphite walls.

3. Near-thermal-equilibrium process

3.1. Source material and seed

The prevailing problem with SiC is still the insufficient crystal quality of the substrates grown by the PVT technique. Hollow tube-shaped defects termed 'micropipes', which grow favourably along the stacking sequence (*c*-axis) of the polytype, still limit the use of SiC for high power devices. Micropipes are in general caused by internal stress. Internal stress can have manifold origins, e.g. screw dislocations providing a large Burgers vector [20, 21] (see figure 5), Si droplets or dust particles at the growth front, large temperature gradients or polytype fluctuations. In the latter case, internal stress is caused by the small deviations in the lattice constants of the different polytypes.

In order to avoid or at least to strongly reduce the density of micropipes, we have developed the 'near-thermal-equilibrium growth (NTEG)' [22]. A brief description of the NTEG 6H-SiC is given in the following: as source material we employed commercially available SiC powder of grain size smaller than 7 μm and mixed it with up to 10% silicon (Si) powder. Prior to

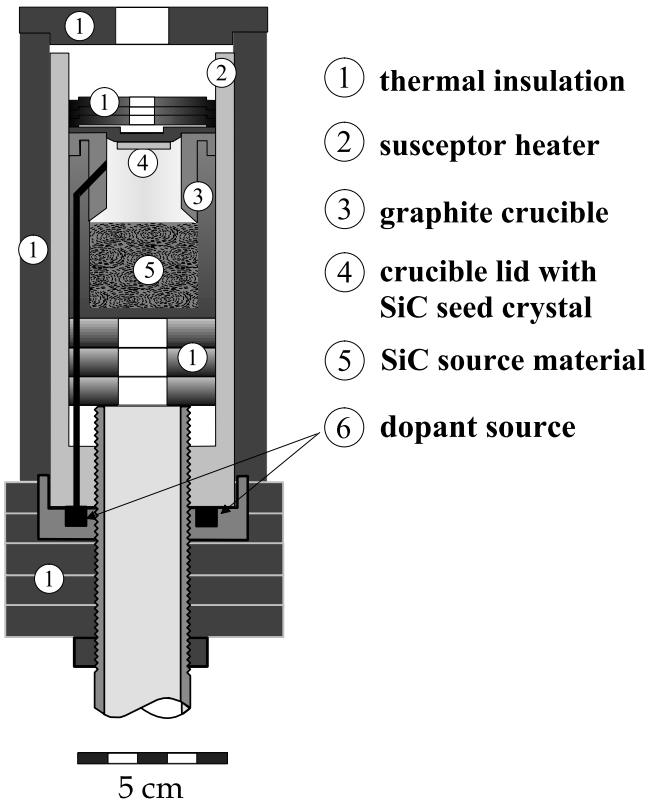

Figure 4. Set-up of the hot zone for the growth of doped SiC single crystals (after [18]).

the growth run, the source material is degassed under vacuum at about 1400 °C and is finally baked out at 2200 °C for 15 min resulting in a sintered SiC massive load.

With increasing proportion of Si to the SiC source material, the growth rate increases. For a mixture of $R = m_{Si}/(m_{SiC} + m_{Si}) > 10\%$, the grown 6H-SiC crystals contain polycrystalline regions as demonstrated in figure 6 [19].

6H-SiC Lely platelets with a low density of dislocations are used as seed crystals. Both surfaces are mechanically polished and oxidized at 1100 °C for 2 h to remove largely the surface damage and—based on the different oxidation rates [23]—to identify the polarity of the surface ((0001) or $(000\bar{1})$). The polarity of the surface can be significant for the growth of a particular polytype. Finally the oxide is removed from the surfaces and the seed crystal is exposed to a standard clean (acetone, aqua regia, HF, deionized water).

3.2. Typical growth run of a 6H-SiC crystal

In figures 7(a) and (b), the source and seed temperature (T_{source}, T_{seed}) measured at the bottom and at the lid of the crucible, respectively, and the argon pressure p_{Ar} are displayed as a function of time during the NTEG. This growth run is subdivided into four steps as indicated by the dashed vertical lines. The result of each step is evaluated by interrupting the growth process at this point and by characterizing the grown crystal with optical microscopy. During step 1 ($T_{source} = 2150$ °C, $T_{seed} = 2150$ °C, $p_{Ar} = 820$ mbar, $t = 1.5$ h) no measurable transport from the source to the lid occurs. However, a significant lateral transport on the seed

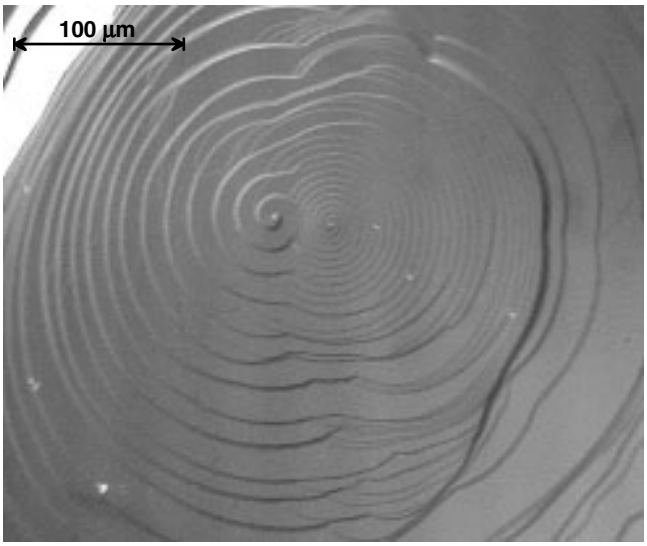

Figure 5. Reflection light image of the as-grown surface of a SiC bulk crystal grown by the sublimation method taken with a Nomarski microscope. Two growth spirals with a significantly different step height (corresponding to the screw component of the Burgers vector) can be observed.

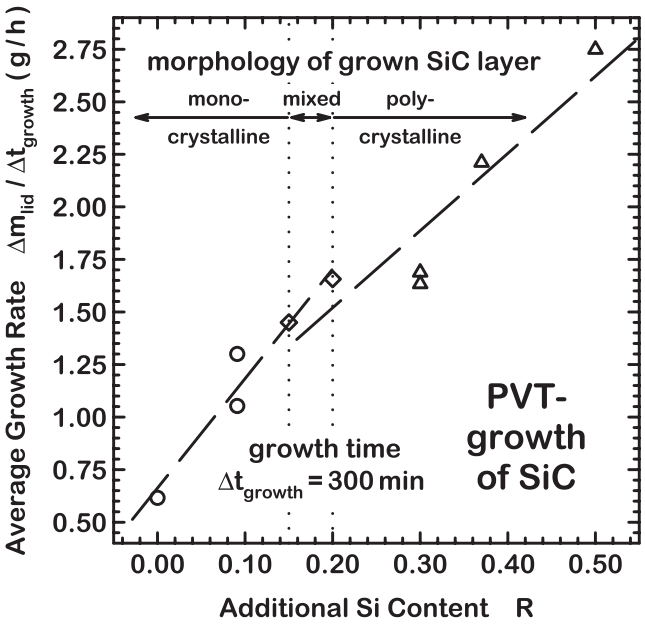

Figure 6. Average SiC growth rate $\Delta m_{\mathrm{lid}}/\Delta t_{\mathrm{growth}}$ as a function of the additional Si content R achieved with PVT growth. Δm_{lid} is the weight of the lid with the crystal attached prior to and subsequent to the crystal growth. The symbols are experimental data and the straight lines correspond to a linear regression to the experimental data (after [19]).

is observed. The growth front adjusts itself to the radial temperature profile in the crucible. In our case, it develops a convex shape. In addition, residual surface defects caused by

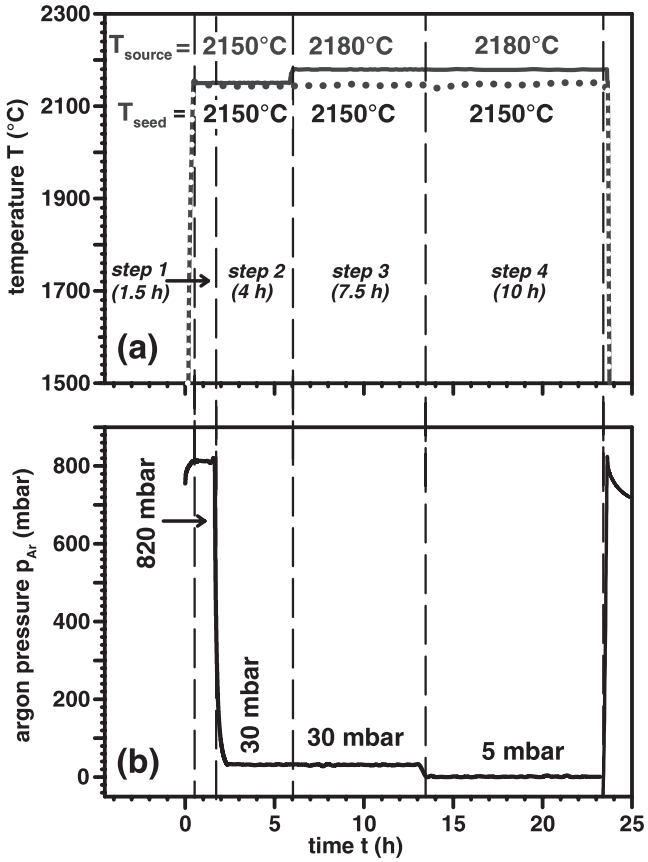

Figure 7. Example of a near-thermal-equilibrium process. Diagrams of (a) the source temperature T_{source} (solid curve), the seed temperature T_{seed} (dotted line) and (b) the argon pressure p_{Ar} as a function of the process time t are shown.

the polishing process disappear and an atomically perfect surface is formed by this slow initial nucleation [24]. During step 2 the argon pressure is reduced ($T_{\text{source}} = 2150\,^{\circ}\text{C}$, $T_{\text{seed}} = 2150\,^{\circ}\text{C}$, $p_{\text{Ar}} = 30$ mbar, $t = 4$ h). Although no temperature gradient between source and seed is established, a growth of 0.9 mm on the seed crystal is achieved. It is assumed that the observed transport of SiC is due to the initially higher partial pressure of Si above the source compared to that above the seed surface. The grown part shows no visible surface defects but a faceted area of about 5 mm in diameter in the centre of the crystal. The establishment of a gradient of 5 K cm^{-1} during step 3 ($T_{\text{source}} = 2180\,^{\circ}\text{C}$, $T_{\text{seed}} = 2150\,^{\circ}\text{C}$, $p_{\text{Ar}} = 30$ mbar, $t = 7.5$ h) does not lead to an enhancement of the growth rate. The source material has apparently lost a high percentage of its Si content during step 2 and after a process time of approximately 7.5 h the growth rate is drastically slowed down. In order to continue with a further growth of the SiC crystal, the argon pressure is reduced to 5 mbar in step 4 ($T_{\text{source}} = 2180\,^{\circ}\text{C}$, $T_{\text{seed}} = 2150\,^{\circ}\text{C}$, $p_{\text{Ar}} = 5$ mbar, $t = 10$ h). Over the total process time of 23 h, an average growth rate of 0.27 mm h^{-1} is reached.

The temperature gradient during the crystal growth is a critical parameter. Figure 8 shows an optical micrograph of a cross-sectional view parallel to the c-axis of a 6H-SiC crystal grown first with a temperature gradient ΔT of 5 K cm^{-1} (layer no 1) and then followed by a growth

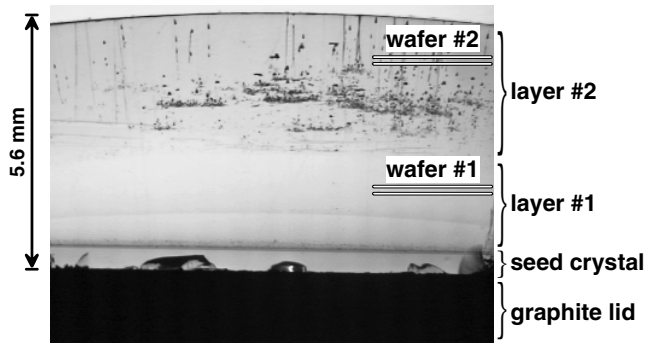

Figure 8. Optical micrograph of a cross-sectional view parallel to the *c*-axis of a 6H-SiC crystal. The inserted lines on the right of the crystal indicate the regions from which wafers no 1 and no 2, used for the micropipe mapping in figure 9, originate.

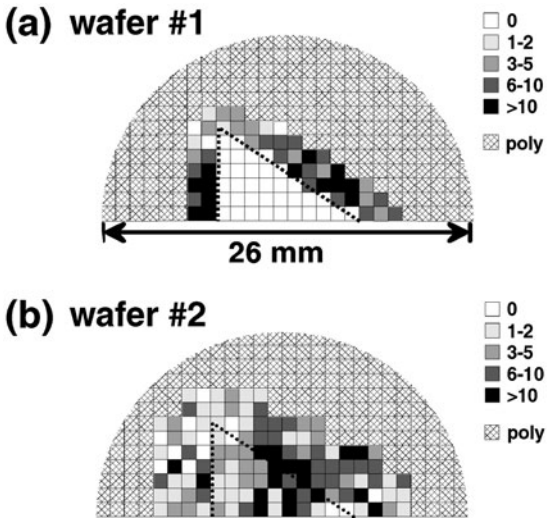

Figure 9. Micropipe mapping of wafers no 1 and no 2 as defined in figure 8. The number of micropipes in a square of 1 mm^2 size is listed in the legend. The area corresponding to the position and the size of the seed crystal is indicated by straight dotted lines. The polycrystalline area is marked by cross-hatched squares.

with $\Delta T = 7.5$ K cm^{-1} (layer no 2). Although the absolute accuracy of the seed and source temperature may be affected by a large error bar, this example demonstrates that there exists only a narrow region for the temperature gradient ΔT, which separates defect-free growth (layer no 1) from the formation of a high density of extended defects (layer no 2). Two wafers (no 1 and no 2) as indicated in figure 8 are cut from this SiC boule and etched in molten KOH at 450 °C for 30 min, in order to decorate individual micropipes [25]. The corresponding micropipe mapping of wafers no 1 and no 2 is shown in figure 9. The number of micropipes is counted in a square of size 1 mm^2. The cross-hatched squares indicate the polycrystalline area, which is grown outside the seed crystal. The area which corresponds to the position of the seed crystal is marked by dotted straight lines. Wafer no 1 provides a complete micropipe-free area over the seed crystal, while wafer no 2 shows a high density of micropipes (average density $\approx$200 micropipes cm^{-2}). As demonstrated above, the NTEG using small temperature

Table 1. Essential growth parameters for the stable growth of 4H-, 15R-, 6H- and 3C-SiC single crystals.

Growth parameter	4H-SiC H = 50%	15R-SiC H = 40%	6H-SiC H = 33%	3C-SiC H = 0%
Seed crystal polytype	4H	15R	6H/15R/21R	3C
Seed face polarity	C face	Si face	Si/C face	(001)
Seed crystal orientation	on/8° off axis	on axis	on axis	on axis
Initial seed to source distance (mm)	30	30	30	5–10
Si addition to the source	0%	0%	10%	Separate Si source at $T \approx 1500\,^{\circ}\mathrm{C}$
Seed temperature (°C)	2100–2180	2150–2180	2100–2250	1850–2000
Temperature gradient (K cm^{-1})	$\leqslant 5$	$\leqslant 5$	$\leqslant 5$	$\leqslant 3.5$
Argon pressure (mbar)	5–820	5–820	5–820	0.5–820
Growth rate (mm h^{-1})	$\leqslant 0.27$	$\leqslant 0.2$	$\leqslant 0.27$	$\leqslant 0.1$
	⟶ Decreasing hexagonality H			

gradients results in a high crystal quality of the grown SiC boules; its disadvantage is the low growth rate of about 0.3 mm h^{-1}, which is up to five times smaller than that of a standard PVT growth with temperature gradients in the range of 20–30 K cm^{-1}.

4. Growth of a particular SiC polytype

The stable and reproducible NTEG of a particular SiC polytype is one of the major aims. There are many different growth parameters which affect the growth of SiC polytypes, e.g. C to Si ratio in the gas phase, T_{source}, T_{seed}, $\Delta T = T_{\mathrm{seed}} - T_{\mathrm{source}}$, p_{Ar}, polarity of the seed crystal and also the geometry and the material of the crucible. Some of these parameters are not independently adjustable but are connected to each other. Because of the fact that the driving force for the growth of a particular SiC polytype is not theoretically understood yet, it is still an experimental puzzle to optimize these parameters. A helpful tool is the 'dual-seed-crystal' method [19] (see figure 10) using two or even more seed crystals with differing properties (e.g. different surface polarity, different polytype or different off-axis orientation), which are subjected to identical growth runs. Table 1 summarizes some of the essential parameters leading to a stable growth of the 4H-, 6H-, 15R- and 3C-SiC polytypes; these results are based on a great number of growth experiments. A stable growth of 4H-SiC crystals could only be achieved on the $(000\bar{1})$-surface of 4H-SiC seed crystals in a narrow temperature range as listed in table 1 (see also [26]).

An important parameter is the C to Si ratio in the vapour phase, which can be adjusted by the composition of the source material. It turns out (see sixth line in table 1) that with increasing Si content the growth of SiC polytypes with decreasing hexagonality H (6H- and 3C-SiC) is preferred. The hexagonality H is given by $N_{\mathrm{h}}/(N_{\mathrm{h}} + N_{\mathrm{k}})$, where N_{h} and N_{k} correspond to the number of inequivalent hexagonal and cubic lattice sites of the particular SiC polytype. This

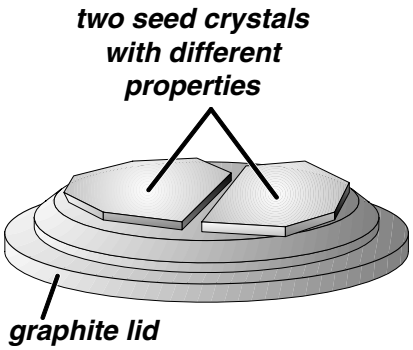

Figure 10. Dual-seed method: two seed crystals are mounted side by side on the lid and can be exposed to identical growth runs.

trend has been confirmed by calculations based on thermodynamic nucleation conducted by Fissel [27] and by low energy electron diffraction (LEED) and scanning tunnelling microscopy (STM) investigations of the reconstruction of SiC surfaces performed by Starke *et al* [28, 29]. The latter authors showed that the cubic stacking sequence is promoted in a Si rich vapour phase.

Because of the high Si vapour pressure and the fact that the growth vessel is not completely sealed, the Si to C ratio in the gas phase decreases with proceeding growth time. In order to keep this ratio constant, a Si containing gas (e.g. silane) can be fed into the growth vessel to compensate the loss of Si from the solid source; this growth technique is termed 'modified PVT growth' in the literature [30].

Takahashi and Ohtani [31] have used seed crystals with the large surfaces perpendicular to the *c*-axis ($[1\bar{1}00]$- or $[11\bar{2}0]$-direction). Such surfaces have stored the information on the particular polytype. The grown SiC crystals perfectly reproduce the polytype of the seed crystal and, in addition, the generation of micropipes is completely avoided. However, a high density of stacking faults is introduced during this growth.

5. Doping of SiC during crystal growth

5.1. Incorporation of donors

The prevailing shallow donor species in SiC crystals is nitrogen (N), which is unintentionally incorporated during the growth process at C lattice sites [32]. In this way, concentrations between 10^{17} cm^{-3} and a few 10^{18} cm^{-3} are reached. The source for the N_2 gas is the residual ambient and the N, which is desorbed from the porous graphite parts of the crucible at the growth temperature. The concentration of N donors can be increased by a controlled addition of N_2 gas during the growth. If the N_2 gas supply is switched on and off, the highly N-doped layers may serve as interface markers [33]. Depending on the SiC polytype, the lattice site (cubic or hexagonal) and the N donor concentration, the ionization energy of N donors varies between 20 and 150 meV [34]. Ohtani *et al* [35] and Schulz *et al* [36] have demonstrated that there is an upper limit of $(3–5) \times 10^{19}$ cm^{-3} for the incorporation of electrically active N donors in 4H-/6H-SiC by the PVT method. If higher N concentrations are chemically incorporated during the growth, the corresponding wafers exhibit high internal stress and brittleness [36]. At concentrations above 10^{19} cm^{-3}, N atoms apparently start to form electrically inactive precipitates.

In order to investigate the influence of the polarity of the seed face—either the Si face (0001) or the C face (000$\bar{1}$)—on the incorporation of N donors, the dual-seed-crystal method (see figure 10) is applied, which enables the simultaneous growth on two different faces under identical conditions. It turns out that the concentration of N donors observed in crystals grown on the C face is higher by approximately a factor of three than in crystals grown on the Si face regardless of the polytype [19].

Laube *et al* [37] have shown by implantation of phosphorus (P) ions into 4H-SiC that this donor species reaches electrically active donor concentrations above 10^{20} cm^{-3}. P donors occupy Si lattice sites [38]; their ionization energies are close to the corresponding quantities of N donors [37]. In order to minimize the electrical losses in vertical high power devices, the availability of SiC substrates with extremely low resisitivity is required. We have, therefore, tried to incorporate P donors at high concentrations during the PVT growth [39]. Pyrophosphate (SiP_2O_7) has been employed as a solid P source. This P compound dissociates into SiO_2 and P_2O_5 at temperatures around 900 °C. Due to the high vapour pressure of P_2O_5, the P source has to be kept at temperatures significantly lower than the SiC source material ($\approx$1300 °C). We have grown several P-doped 6H-SiC crystals and tested different arrangements of the P source. Secondary ion mass spectrometry (SIMS) analyses of the corresponding SiC boules resulted in a chemical P concentration of 3×10^{17} cm^{-3}. We suggest that P atoms form stable molecules in the gas phase or react with C at temperatures above 1600 °C. In this way, the incorporation of a desirable high P concentration into SiC is prevented. Similar results are obtained from P-doping experiments using phosphine during the chemical vapour deposition (CVD) process [40]. P doping of SiC during the PVT and CVD growth is still an unsolved problem.

5.2. Incorporation of acceptors

Aluminium (Al) and boron (B) atoms residing at the Si sublattice of SiC act as acceptors [32]; their ionization energies are roughly 200 and 300 meV, respectively, independent of the polytype and of the lattice site (cubic or hexagonal) [34]. Boron is a common contamination in graphite and is unintentionally incorporated during the PVT growth at lower concentrations in the range of 10^{16}–10^{17} cm^{-3}. In n-type SiC crystals, these B acceptors dominate the compensation. Because of the smaller ionization energy Al is the preferred acceptor species for device applications. In order to achieve p-type conductivity in SiC, the background concentration of N donors has to be overcompensated.

In order to dope SiC during the PVT growth with Al acceptors, we used Al_4C_3 powder as the Al source [41]. Because of the high partial pressure of Al for all the suitable Al compounds [42] (see figure 11) the Al source is kept in a separate graphite container providing diffusion channels for the Al into the growth crucible (see figure 4). In this arrangement, the temperature of the Al source is approximately 1600 °C. In figure 12, the electrically active Al acceptor concentration is monitored by Hall effect and CV investigations; the chemical Al concentration is determined by SIMS. The different measurement points are obtained from samples which are cut from an Al-doped 6H-SiC boule perpendicular to the growth direction. The Al acceptor concentration and the resistivity at room temperature vary in the ranges (0.4–1) $\times$ 10^{19} cm^{-3} and 0.8–1.5 Ω cm, respectively, as a function of the distance from the seed crystal. The Al acceptor concentration in figure 12 does not decrease towards the tail of the SiC boule, demonstrating that the Al source is not exhausted during the growth run.

Al-doped 4H-/6H-SiC crystals have been grown side by side on Si and C faces. SIMS measurements reveal that the incorporation rate of Al into Si faces is approximately twice as high as in C faces, which is opposite to the incorporation of N atoms. Consequently the Si face has to be selected as the growth front to reach high Al acceptor concentrations.

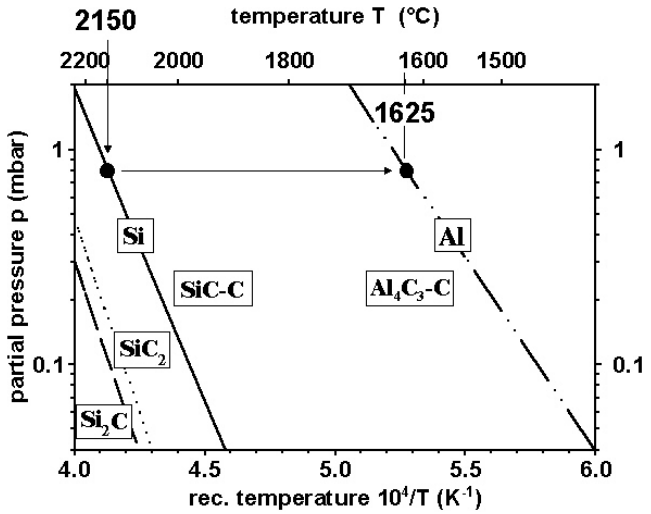

Figure 11. Temperature dependence of the partial pressure p of several vapour phase constituents above SiC in the SiC–C equilibrium (after [10]) and vapour pressure of aluminium above Al_4C_3 powder in the Al_4C_3–C system (after [41]). The curves are obtained from a least-squares fit of the Clausius–Clapeyron equation to experimental data.

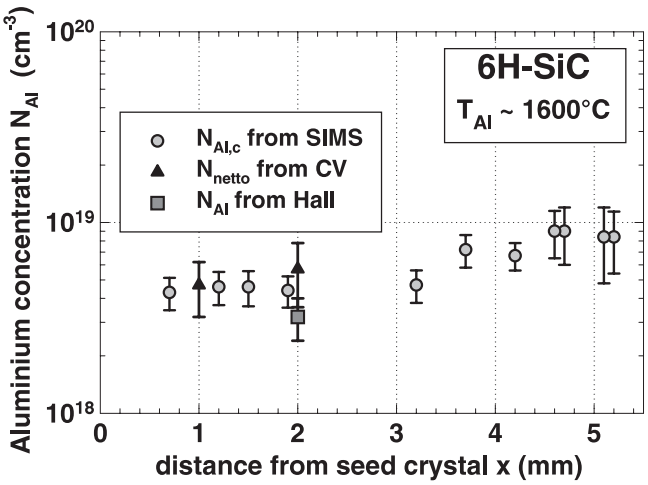

Figure 12. Aluminium concentration N_{Al} of a 6H-SiC crystal as a function of distance from the seed crystal x obtained by SIMS, CV and Hall effect measurements (for corresponding symbols see the inset).

6. Conclusion and outlook

As demonstrated, the PVT technique provides a suitable tool to grow reproducibly 4H- and 6H-SiC single crystals of high polytype purity. Based on its favourable electronic properties, the growth of 3C-SiC boules is extremely desirable. Although the feasibility of its growth by the PVT technique is demonstrated, the crystal quality is still poor; in addition, such 3C-SiC crystals are not yet commercially available. During the last few years strong progress has been achieved in extending the diameter of 4H-/6H-SiC wafers (see figure 13)

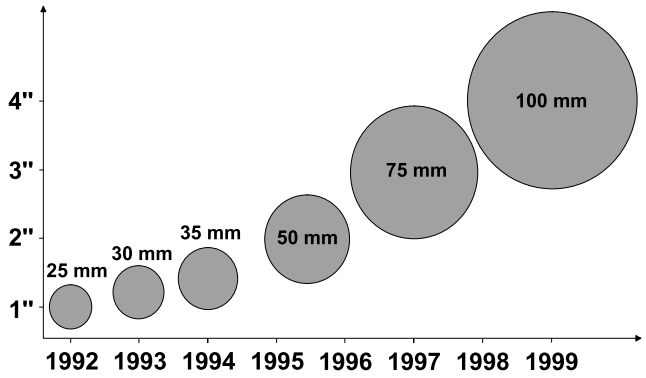

Figure 13. Increase in R&D 4H-SiC wafer diameter versus year (after [43]).

and in reducing extended crystal defects like micropipes and inclusions [43]. At present, 4H- and 6H-SiC wafers 3 inches in diameter and a standard/ultra-low micropipe density of (30–100)/$\leqslant$5 micropipes cm^{-2} are commercially available. The doping levels of donors and acceptors can be adjusted in the ranges (10^{17}–3×10^{19}) and (10^{18}–5×10^{19}) cm^{-3}, respectively.

The ongoing work has to be focused on a further extension of the wafer diameter—wafers 4 inches in diameter have already been demonstrated—and in a strong reduction of extended crystal defects. Regarding these defects, the dislocation and stacking fault density also has to be included. A further topic will be the growth of semi-insulating SiC, which is not based on the compensation by extrinsic impurities like vanadium, but on thermally stable intrinsic defects. First results in growing pure high-resistivity SiC crystals are already available; however, there is still a lack of physical understanding of this compensating mechanism.

Acknowledgment

The support of this work by the German Science Foundation (SiC-Forschergruppe) is greatly acknowledged.

References

[1] Cowless A H and Cowless E H 1885 *US Patent Specification* 319945
[2] Acheson A G 1892 *English Patent Specification* 1711
[3] Knippenberg W F 1963 *Philips Res. Rep.* **18** 161
[4] Lely J A 1955 *Ber. Dtsch. Keram. Ges.* **32** 229
[5] Hergenrother K M, Mayer S E and Mlavsky A I 1960 *Proc. Conf. on Silicon Carbide* ed J R O'Connor and J Smiltens (Boston, MA: Pergamon) p 60
[6] Tairov Y M and Tsvetkov V F 1978 *J. Cryst. Growth* **43** 209
[7] Ziegler G, Lanig P, Theis D and Weyrich C 1983 *IEEE Trans. Electron Devices* **30** 277
[8] Augustine G, Hobgood H McD, Balakrishna V, Dunne G and Hopkins R H 1997 *Phys. Status Solidi* b **202** 137
[9] Vodakov Yu A, Roenkov A D, Ramm M G, Mokhov E N and Makarov Yu N 1997 *Phys. Status Solidi* b **202** 177
[10] Drowart J, DeMaria G and Inghram M G 1958 *J. Chem. Phys.* **29** 1015
[11] Lilov S K 1995 *Diamond Relat. Mater.* **4** 1331
[12] Faktor M M and Garrett T 1974 *Growth of Crystals from the Vapour* (London: Chapman and Hall)
[13] Schönherr E 1980 *Growth Prop. Appl. Crystallogr.* **2** 51
[14] Hofmann D, Heinze M, Winnacker A, Durst F, Kadinski L, Kaufmann P, Makarov Yu N and Schäfer M 1995 *J. Cryst. Growth* **146** 214
[15] Matsunami H 1993 *Physica* B **185** 65
[16] Tairov Y M and Tsvetkov V F 1979 *J. Cryst. Growth* **46** 403

[17] Heydemann V D 1996 *Dissertation* Erlangen
[18] Schulze N, Gajowski J, Semmelroth K, Laube M and Pensl G 2001 *Mater. Sci. Forum* **353–356** 45
[19] Heydemann V D, Schulze N, Barrett D L and Pensl G 1996 *Appl. Phys. Lett.* **69** 3728
[20] Frank F C 1951 *Acta Crystallogr.* **4** 497
[21] Heindl J, Strunk H P, Heydemann V D and Pensl G 1997 *Phys. Status Solidi* a **162** 251
[22] Schulze N, Barrett D L and Pensl G 1998 *Appl. Phys. Lett.* **72** 1632
[23] von Münch W and Pfaffeneder I 1975 *J. Electrochem. Soc.* **122** 642
[24] Heydemann V D, Rohrer G S, Sanchez E K and Skowronki H 1998 *Mater. Sci. Forum* **264–268** 37
[25] Takahashi J, Kanaga M and Hoshimo T 1993 *Inst. Phys. Conf. Ser.* **137** 13
[26] Stein R A, Lanig P and Leibenzeder S 1992 *Mater. Sci. Eng.* B **11** 69
[27] Fissel A 2000 *J. Cryst. Growth* **212** 438
[28] Starke U, Schardt J, Berhardt J, Franke M and Heinz K 1999 *Phys. Rev. Lett.* **82** 2107
[29] Starke U, Bernhardt J, Schardt J, Seubert A and Heinz K 2000 *Mater. Sci. Forum* **338–342** 341
[30] Straubinger T L, Bickermann M, Weingärtner R, Wellmann P J and Winnacker A 2002 *J. Cryst. Growth* **240** 117
[31] Takahashi J and Ohtani N 1997 *Phys. Status Solidi* b **202** 163
[32] Greulich-Weber S 1997 *Phys. Status Solidi* a **162** 95
[33] Eckstein R, Hofmann D, Makarov Y, Müller St G, Pensl G, Schmitt E and Winnacker A 1996 *Mater. Res. Soc. Symp. Proc.* **423** 215
[34] Pensl G and Choyke W J 1993 *Physica* B **185** 264
[35] Ohtani N, Katsuno M, Takahashi J, Yashiro H and Kanaya M 1998 *J. Appl. Phys.* **83** 4487
[36] Schulz D, Irmscher K, Dolle J, Eisenbeck W, Müller T, Rost H-J, Siche D, Wagner G and Wollweber J 2000 *Mater. Sci. Forum* **338–342** 87
[37] Laube M, Schmid F, Pensl G, Wagner G, Linnarsson M and Maier M 2002 *J. Appl. Phys.* **92** 549
[38] Kalabukhova E N, Lukin S N and Mokhov E N 1993 *Phys. Solid State* **35** 361
[39] Semmelroth K, Schmid F, Karg D, Pensl G, Maier M, Greulich-Weber S and Spaeth J-M 2003 *Mater. Sci. Forum* **433–436** 63
[40] Wang R, Bhat I B and Chow T P 2002 *J. Appl. Phys.* **92** 7587
[41] Schulze N, Gajowski J, Semmelroth K, Laube M and Pensl G 2001 *Mater. Sci. Forum* **353–356** 45
[42] Qiu C and Metselaar R 1994 *J. Alloys Compounds* **216** 55
[43] Carter C H Jr, Glass R, Brady M, Malta D, Henshall D, Müller S, Tsvetkov V, Hobgood D and Powell A 2001 *Mater. Sci. Forum* **353–356** 3